Sensitivity-enhanced multidimensional solid-state NMR spectroscopy by optimal-control-based transverse mixing sequences

Jan Blahut[1,2], Matthias Brandl[3], Tejaswini Pradhan[3], Bernd Reif[3,4,*], Zdeněk Tošner[1,*]

[1]Department of Chemistry, Faculty of Science, Charles University, Albertov 6, 12842 Prague, Czech Republic

[2]Institute of Organic Chemistry and Biochemistry of the CAS, Flemingovo nám. 2, 16610, Prague, Czech Republic

[3]Bayerisches NMR Zentrum (BNMRZ) at Department Chemie, Technische Universität München (TUM), 85747 Garching, Germany

[4]Helmholtz-Zentrum München (HMGU), Deutsches Forschungszentrum für Gesundheit und Umwelt, 85764 Neuherberg, Germany

*Corresponding authors:

- Zdeněk Tošner, zdenek.tosner@natur.cuni.cz
- Bernd Reif, reif@tum.de

Graphical abstract

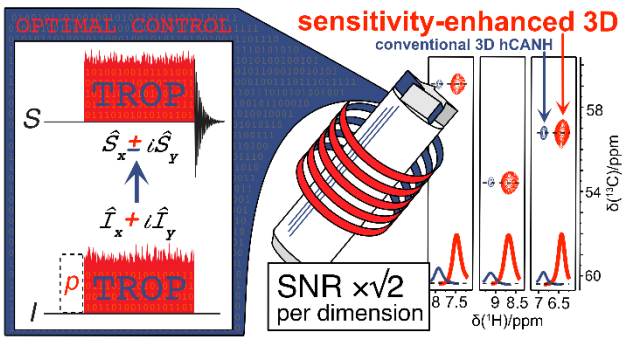

Abstract

Recently, proton-detected magic-angle spinning (MAS) solid-state nuclear magnetic resonance (NMR) spectroscopy has become an attractive tool to study the structure and dynamics of insoluble proteins at atomic resolution. The sensitivity of the employed multidimensional experiments can be systematically improved when both transversal components of the magnetization are transferred simultaneously after an evolution period. The method of preservation of equivalent pathways has been explored in solution-state NMR; however, it does not find widespread application due to relaxation issues connected with increased molecular size. We present here for the first time heteronuclear transverse mixing sequences for correlation experiments at moderate and fast MAS frequencies. Optimal control allows to systematically boost the signal-to-noise ratio (SNR) beyond the expected factor of $\sqrt{2}$ for each indirect dimension. In addition to the carbon-detected sensitivity-enhanced 2D NCA experiment, we present a novel proton-detected, doubly sensitivity-enhanced 3D hCANH pulse sequence for which we observe a 3-fold improvement in SNR compared to the conventional experimental implementation. The sensitivity gain turned out to be essential to unambiguously characterize a minor fibril polymorph of a human lambda-III immunoglobulin light chain protein that escaped detection so far.

Nuclear magnetic resonance (NMR) is a versatile technique with a wide range of applications in chemistry. In structural biology, solid-state NMR has recently reached a similar level as solution-state NMR and has been used recently to determine the structure of insoluble proteins such as amyloids fibrils,[1,2] cytoskeleton associated factors,[3] phage coat or tail spike proteins,[4,5] and membrane proteins.[6,7] This advance has been enabled by the recent progress in sample preparation including various isotope labeling strategies,[8] development of fast magic-angle-spinning (MAS) hardware[9] yielding more efficient averaging of anisotropic interactions,[10] and the availability of ultrahigh magnetic fields resulting in increased resolution and sensitivity.[11] In analogy to solution-state NMR, numerous proton-detected multidimensional solid-state NMR experimental schemes have been developed[12–14] to increase the effective resolution and to resolve the massive overlap of resonances in large protein systems. However, sensitivity remains the major obstacle for a broader applicability, in particular in the solid-state, due to the integrated loss of sensitivity in the multiple magnetization transfer elements in high-dimensional pulse schemes. Evolution periods are used to encode the chemical shift information of a particular nucleus (spin *I*) into the phase of the coherence, reflected by the two transverse magnetization components directed along the *x* and *y* axes (Figure 1). Conventionally, only one magnetization component is selected and transferred to the coupled nucleus (spin *S*), while the second component is not recovered. Chemical shifts are encoded in modulations of the signal amplitude. This selection results in a reduction of the signal-to-noise ratio (SNR) by a factor of $2^{(N-1)/2}$ in a general N-dimensional correlation experiment. In solution-state NMR, 'sensitivity-enhanced' implementations of 2D experiments have been developed, where both transverse magnetization components are transferred from spin *I* to *S*. There, the chemical shift information is encoded in modulations of the signal phase. This technology has been denoted 'preservation of equivalent pathways' (PEP)[15] or 'coherence order selective' (COS)[16] transfers. In the heteronuclear correlation experiment, two successive INEPT-like refocusing elements are used. To transfer both the *x* and *y* component, one component is intermittently stored as longitudinal magnetization while the other component is preserved as multiple-quantum coherence.[17] The duration of such a PEP/COS transfer scheme is increased by a factor of two which yields a loss of intensity due to relaxation especially for large protein complexes. As a consequence, the SNR in a doubly sensitivity-enhanced 3D HNCO experiment recorded for the protein rhodniin (103 amino acids) is improved only by a factor of 1.22 instead of the expected two-fold gain.[18] Similar homonuclear correlation experiments (TOCSY) can make use of an isotropic mixing Hamiltonian that is active during the spinlock transfer.[19]

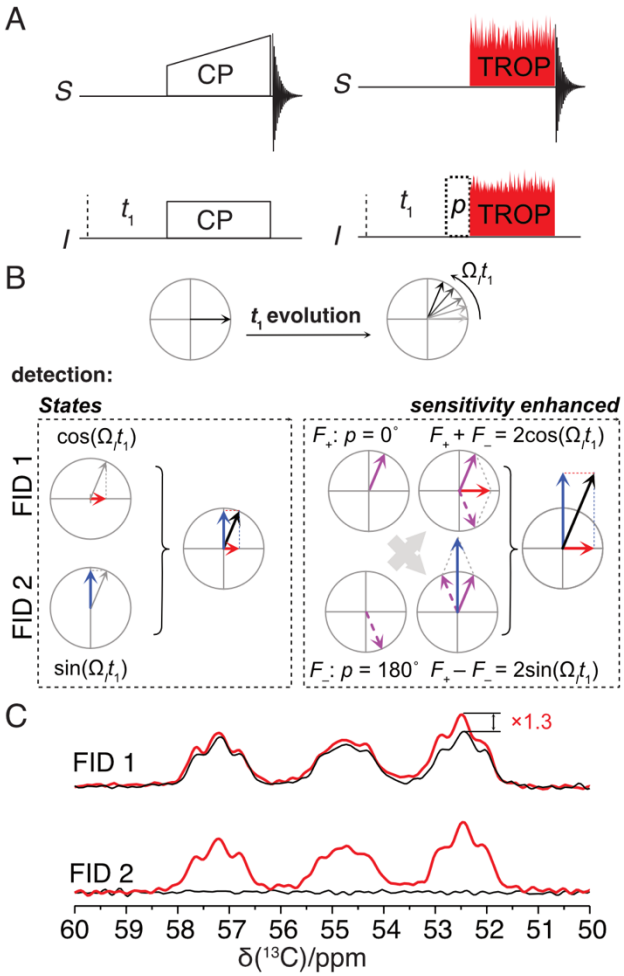

Figure 1. Principle of sensitivity enhancement. (A,B) Two components have to be acquired in the indirect evolution period for each t_1 increment to yield sign discrimination of frequencies and phase -sensitive spectra.[20] In the States acquisition scheme,[21] the cosine and sine modulated signals (FID 1 and FID 2) are obtained by transferring the real and imaginary component sequentially. In sensitivity-enhanced experiments, two phase-modulated FIDs are recorded that are associated with echo F_+ and anti-echo F_- pathways,[16] (that can be discriminated by the 180°-pulse *p*). The two FIDs are added and subtracted to yield the cosine and sine modulated signals with a two-fold higher amplitude. Due to noise accumulation, the SNR is increased by a factor of $\sqrt{2}$. (C) Experimental spectra obtained for the two components recorded for the increment t_1=0. For ramp-CP, only the cosine modulated FID contains signal (FID 1, black), while there is signal in both F_+ and F_- FIDs after the TROP pulse (red). In addition, TROP benefits from compensation of rf inhomogeneities yielding improved efficiency. The spectra show the Cα resonances of a microcrystalline f-MLF peptide sample. Experimental details are provided in the Supporting information.

Most of the magnetization transfer techniques in solid-state NMR developed so far have been designed to transfer only a single component. It includes the most popular cross-polarization experiment employed as a standard building block in multidimensional experiments. The potential of sensitivity enhancement by the PEP scheme has been largely overlooked in solid-state NMR, with a few exceptions.[22–30] Gopinath and co-workers[25–27] presented sensitivity-enhanced experiments to measure dipolar couplings in static and oriented samples. In rotating solids, Tycko[24] suggested a sensitivity-enhanced 2D carbon-carbon correlation experiment using a finite pulse radio-frequency-driven recoupling[31] at a MAS frequency of 25 kHz. Khaneja et al.[28,29] introduced theoretically the so called γ-preparation scheme that combines modulation of the coherence phase by chemical shifts with the crystallite orientation dependency during the magnetization transfer. Tošner et al.[30] used optimal control to design an effective isotropic mixing Hamiltonian in a ^{13}C homonuclear spin system. So far, however, there is no study in the literature devoted to sensitivity-enhanced proton detected heteronuclear correlations at fast MAS frequencies that yields significant gains in sensitivity routinely.

In this communication, we introduce shaped pulses developed by means of optimal control for the simultaneous transfer of both transverse magnetization components in heteronuclear correlation spectroscopy. The duration of the transfer periods is the same as the duration of the magnetization transfer elements in the conventional counterparts. The **Tr**ansverse mixing **O**ptimal control **P**ulses (TROP) can be integrated into any multidimensional experiment and do provide a gain in sensitivity of $>\sqrt{2}$ per each indirect dimension. Data can be processed using standard NMR spectrometer software employing the already existing implementations from solution-state NMR. TROP elements were numerically optimized using the GRAPE algorithm[32] implemented in SIMPSON[33–35] as described in our previous studies.[36,37] The optimization procedure accounts for spatial rf field inhomogeneity[36,38] and allows the resulting pulse shapes to be adjusted to a particular MAS frequency of the experiment.[37] Possible imbalance of the x and y pathways is compensated by a two-step phase cycle.[39] All details of the theory and the pulse sequence optimization are provided in the Supporting information.

The sensitivity-enhanced ^{13}C detected 2D hNCA experiment with ^{15}N,^{13}C TROP pulses yield a 1.6-1.8x higher sensitivity than the conventional 2D scheme at a MAS frequency of 20 kHz and using the tripeptide sample f-MLF (Figure 2A). In the reference experiment, a carefully optimized ramp-CP was used for the ^{15}N,^{13}C transfer. The PEP scheme provides $\sqrt{2}$ improvement and the remaining factor of about 1.2 is attributed to the higher transfer efficiency of the optimal control TROP pulses that account for inhomogeneous rf fields. For fast MAS (55 kHz), we implemented a 3D se-hCANH experiment with ^{1}H detection using ^{13}C,^{15}N and ^{15}N,^{1}H TROP pulses. Using a perdeuterated and amide proton back-exchanged microcrystalline sample of the chicken α-spectrin SH3 domain, we find that the SNR increased by an average factor of 1.8 ± 0.2 in se-hCANH spectrum compared to the conventional scheme with ramp-CP (^{1}H,^{13}C and ^{15}N,^{1}H) and tm-SPICE (^{13}C,^{15}N) transfer elements (Figure 2B,C; see also Supporting information).

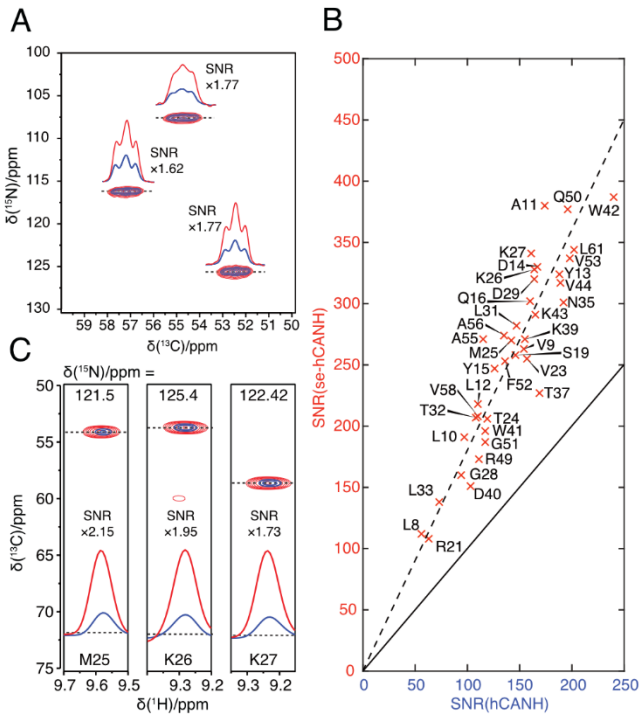

Figure 2: Comparison of spectra obtained from multidimensional sensitivity-enhanced optimal-control-based experiments (red) and their conventional counterparts (blue). (A) Carbon-detected 2D se-hNCA spectrum of the f-MLF peptide acquired using a MAS frequency of 20 kHz. Insets with 1D spectra show slices along the ^{13}C dimension taken at the position indicated by the dashed lines. The numbers show the gains in signal-to-noise ratio (SNR) (B) Peak-specific improvement of SNR in the proton-detected 3D se-hCANH spectrum recorded for a microcrystalline SH3 protein sample (perdeuterated and back-exchanged), setting the MAS frequency to 55 kHz. The dashed line represents the average SNR improvement by a factor of 1.8. The 3D spectrum in (C) is presented as a 2D taken at the ^{15}N chemical shift indicated at the top. The data confirms that sensitivity improvements are feasible beyond the canonical factor of $\sqrt{2}$ per indirect dimension. Experimental details are given in the Supporting information.

To demonstrate that the approach is suitable for applications, we applied the sensitivity-enhanced 3D experiments to an amyloid fibril sample formed by the patient derived light chain antibody variable domain protein FOR005.[40] Cryo-EM fibril reconstructions of this protein yield two different conformations[41] which are distinct in the length of an ill-defined loop and which are populated at a ratio of approximately 2:1 (PDB ID 6Z10 and 6Z1I, Figure 3A). The first polymorph shows no defined density for residues R49-R60, while the region involving residues R49-N68 is not well resolved in the second polymorph. The two polymorphs occur in a single filament and are a consequence of so-called structural breaks. These structural breaks are thought to be related to amyloid fibril branching and of secondary nucleation,[42] and are thus of high interest for the amyloid community. The solid-state NMR sample has been prepared using *ex vivo* seeds to imprint the native fibril structure on the biochemically produced isotopically labeled protein. It has been shown that the core of the solid-state NMR structure is highly similar to the cryo-EM reconstruction.[43] In ^{13}C based assignment experiments, no second polymorph could be detected so far. The heterogeneous region is close in space to the C-terminus which contains a triple glycine sequence element. The glycines pack against the polymorphic region and sense fibril polymorphism. In the proton detected ^{1}H,^{15}N correlation experiments (Fig. 3B) additional cross peaks are observed that could not be sequentially assigned so far due to lack of sensitivity. Figures 3C,D show comparison of the conventional and sensitivity-enhanced 3D hCANH experiments. The trace along the carbon dimension (Figure 3E) indicates that the sensitivity increases on the order of 3-fold in comparison to the conventional 3D hCANH experiment. While more work is necessary to yield a fundamental understanding of the structure and dynamics of this region in the amyloid fibril, our experiments provide the groundwork that will enable a detailed NMR spectroscopic characterization of these systems in the future.

In this paper, we described multidimensional sensitivity-enhanced experiments for solid-state NMR applications on protein samples. While in liquids the magnetization transfer efficiency decreases exponentially with the molecular size due to increased relaxation in INEPT-like transfers, the polarization transfer efficiency in solid state is independent of the molecular size as the coherence lifetimes are not given by molecular tumbling. Our TROP transfer elements do not lead to any relaxation losses and yield enhancement factors higher than the canonical $\sqrt{2}$ for each indirect dimension. As such, they can be readily expanded to arbitrary dimensionality and are fully compatible with non-uniform sampling schemes. We foresee the importance of transverse mixing for implementation of just emerging[44] 5D spectra for which the SNR can be improved by a factor of 4 (a factor of 16 savings in the acquisition time).

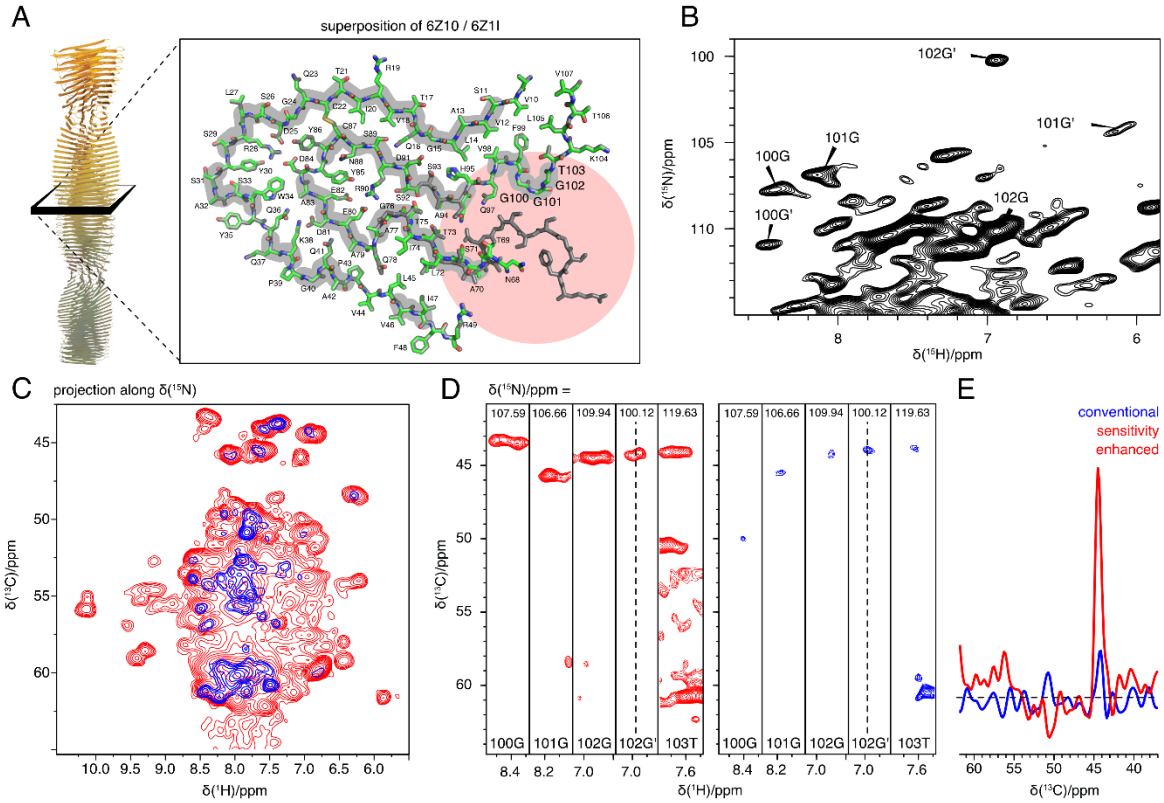

Figure 3. Observation of a second polymorph in an AL amyloid fibril enabled by sensitivity enhancement. (A) Structural model of a FOR005 light chain amyloid fibril.[41] The cryo-EM study reveals two polymorphs for residues R60-T69 within a single protofibril that are populated at a ratio of approximately 2:1 (indicated with a red shaded circle) (PDB ID: 6Z1O/ 6Z1I). Sequentially assigned residues are highlighted in grey. (B) Selected region of a 2D ^{1}H,^{15}N correlation spectrum highlighting cross peaks of glycine residues in the C-terminal region that yields two sets of resonances. The second polymorph is indicated with dashes. (C) Comparison of the sensitivity-enhanced (red) and conventional (blue) 3D hCANH correlation spectra, displayed as a 2D map with the collapsed ^{15}N dimension. Contour levels are set to the equal noise level. (D) 3D hCANH specra presented as strip plots drawn for residues G100-T103 of the light chain antibody domain. (E) 1D traces through the 102G' peaks (indicated by dashed lines in D). Sensitivity enhancement is essential to observe unambiguously the second polymorph. In the sensitivity-enhanced experiment, the signal-to-noise ratio is improved by a factor of ca. 3 in comparison to the conventional acquisition scheme.

Supporting Information

Calculation of TROP elements, pulse sequences, experimental details, and additional experiments using f-MLF sample.

Acknowledgement

This work was supported by the joined project of the German Research Foundation and the Czech Science Foundation (Re/1435-20 and 20-00166J, respectively), and additionally by the Helmholtz-Gemeinschaft. Computational resources were supplied by the Leibniz Supercomputing Centre (Munich), and the project "e-Infrastruktura CZ" (e-INFRA CZ LM2018140) supported by the Ministry of Education, Youth and Sports of the Czech Republic (MEYS CR). We also acknowledge CF NMR of CIISB, Instruct-CZ Centre, supported by MEYS CR (LM2018127)) and European Regional Development Fund-Project „UP CIISB“ (No. CZ.02.1.01/0.0/0.0/18_046/0015974).

References

(1) Daskalov, A.; Martinez, D.; Coustou, V.; El Mammeri, N.; Berbon, M.; Andreas, L. B.; Bardiaux, B.; Stanek, J.; Noubhani, A.; Kauffmann, B.; Wall, J. S.; Pintacuda, G.; Saupe, S. J.; Habenstein, B.; Loquet, A. Structural and Molecular Basis of Cross-Seeding Barriers in Amyloids. *Proc. Natl. Acad. Sci.* **2021**, *118* (1), e2014085118. https://doi.org/10.1073/pnas.2014085118.

(2) Dregni, A. J.; Wang, H. K.; Wu, H.; Duan, P.; Jin, J.; DeGrado, W. F.; Hong, M. Inclusion of the C-Terminal Domain in the β-Sheet Core of Heparin-Fibrillized Three-Repeat Tau Protein Revealed by Solid-State Nuclear Magnetic Resonance Spectroscopy. *J. Am. Chem. Soc.* **2021**, *143* (20), 7839–7851. https://doi.org/10.1021/jacs.1c03314.

(3) Kraus, J.; Russell, R. W.; Kudryashova, E.; Xu, C.; Katyal, N.; Perilla, J. R.; Kudryashov, D. S.; Polenova, T. Magic Angle Spinning NMR Structure of Human Cofilin-2 Assembled on Actin Filaments Reveals Isoform-Specific Conformation and Binding Mode. *Nat. Commun.* **2022**, *13* (1), e2114. https://doi.org/10.1038/s41467-022-29595-9.

(4) Andreas, L. B.; Jaudzems, K.; Stanek, J.; Lalli, D.; Bertarello, A.; Le Marchand, T.; Cala-De Paepe, D.; Kotelovica, S.; Akopjana, I.; Knott, B.; Wegner, S.; Engelke, F.; Lesage, A.; Emsley, L.; Tars, K.; Herrmann, T.; Pintacuda, G. Structure of Fully Protonated Proteins by Proton-Detected Magic-Angle Spinning NMR. *Proc. Natl. Acad. Sci.* **2016**, *113* (33), 9187–9192. https://doi.org/10.1073/pnas.1602248113.

(5) Zinke, M.; Sachowsky, K. A. A.; Öster, C.; Zinn-Justin, S.; Ravelli, R.; Schröder, G. F.; Habeck, M.; Lange, A. Architecture of the Flexible Tail Tube of Bacteriophage SPP1. *Nat. Commun.* **2020**, *11* (1), e5759. https://doi.org/10.1038/s41467-020-19611-1.

(6) Andreas, L. B.; Reese, M.; Eddy, M. T.; Gelev, V.; Ni, Q. Z.; Miller, E. A.; Emsley, L.; Pintacuda, G.; Chou, J. J.; Griffin, R. G. Structure and Mechanism of the Influenza A M2 18–60 Dimer of Dimers. *J. Am. Chem. Soc.* **2015**, *137* (47), 14877–14886. https://doi.org/10.1021/jacs.5b04802.

(7) Schubeis, T.; Le Marchand, T.; Daday, C.; Kopec, W.; Tekwani Movellan, K.; Stanek, J.; Schwarzer, T. S.; Castiglione, K.; de Groot, B. L.; Pintacuda, G.; Andreas, L. B. A β-Barrel for Oil Transport through Lipid Membranes: Dynamic NMR Structures of AlkL. *Proc. Natl. Acad. Sci.* **2020**, *117* (35), 21014–21021. https://doi.org/10.1073/pnas.2002598117.

(8) Chevelkov, V.; Rehbein, K.; Diehl, A.; Reif, B. Ultrahigh Resolution in Proton Solid-State NMR Spectroscopy at High Levels of Deuteration. *Angew. Chemie Int. Ed.* **2006**, *45* (23), 3878–3881. https://doi.org/https://doi.org/10.1002/anie.200600328.

(9) Deschamps, M. Ultrafast Magic Angle Spinning Nuclear Magnetic Resonance. In *Annual Reports on NMR Spectroscopy*; Webb, G. A., Ed.; 2014; Vol. 81, pp 109–144. https://doi.org/10.1016/b978-0-12-800185-1.00003-6.

(10) Bockmann, A.; Ernst, M.; Meier, B. H. Spinning Proteins, the Faster, the Better? *J Magn Reson* **2015**, *253*, 71–79. https://doi.org/10.1016/j.jmr.2015.01.012.

(11) Callon, M.; Malär, A. A.; Pfister, S.; Římal, V.; Weber, M. E.; Wiegand, T.; Zehnder, J.; Chávez, M.; Cadalbert, R.; Deb, R.; Däpp, A.; Fogeron, M. L.; Hunkeler, A.; Lecoq, L.; Torosyan, A.; Zyla, D.; Glockshuber, R.; Jonas, S.; Nassal, M.; Ernst, M.; Böckmann, A.; Meier, B. H. Biomolecular Solid-State NMR Spectroscopy at 1200 MHz: The Gain in Resolution. *J. Biomol. NMR* **2021**, *75* (6–7), 255–272. https://doi.org/10.1007/s10858-021-00373-x.

(12) Barbet-Massin, E.; Pell, A. J.; Retel, J. S.; Andreas, L. B.; Jaudzems, K.; Franks, W. T.; Nieuwkoop, A. J.; Hiller, M.; Higman, V.; Guerry, P.; Bertarello, A.; Knight, M. J.; Felletti, M.; Le Marchand, T.; Kotelovica, S.; Akopjana, I.; Tars, K.; Stoppini, M.; Bellotti, V.; Bolognesi, M.; Ricagno, S.; Chou, J. J.; Griffin, R. G.; Oschkinat, H.; Lesage, A.; Emsley, L.; Herrmann, T.; Pintacuda, G. Rapid Proton-Detected NMR Assignment for Proteins with Fast Magic Angle Spinning. *J. Am. Chem. Soc.* **2014**, *136* (35), 12489–12497. https://doi.org/10.1021/ja507382j.

(13) Stanek, J.; Andreas, L. B.; Jaudzems, K.; Cala, D.; Lalli, D.; Bertarello, A.; Schubeis, T.; Akopjana, I.; Kotelovica, S.; Tars, K.; Pica, A.; Leone, S.; Picone, D.; Xu, Z.-Q.; Dixon, N. E.; Martinez, D.; Berbon, M.; El Mammeri, N.; Noubhani, A.; Saupe, S.; Habenstein, B.; Loquet, A.; Pintacuda, G. NMR Spectroscopic Assignment of Backbone and Side-Chain Protons in Fully Protonated Proteins: Microcrystals, Sedimented Assemblies, and Amyloid Fibrils. *Angew. Chemie Int. Ed.* **2016**, *55* (50), 15504–15509. https://doi.org/doi:10.1002/anie.201607084.

(14) Le Marchand, T.; Schubeis, T.; Bonaccorsi, M.; Paluch, P.; Lalli, D.; Pell, A. J.; Andreas, L. B.; Jaudzems, K.; Stanek, J.; Pintacuda, G. 1 H-Detected Biomolecular NMR under Fast Magic-Angle Spinning. *Chem. Rev.* **2022**, *122* (10), 9943–10018. https://doi.org/10.1021/acs.chemrev.1c00918.

(15) Cavanagh, J.; Rance, M. *Sensitivity-Enhanced NMR Techniques for the Study of Biomolecules*; 1993; Vol. 27. https://doi.org/10.1016/S0066-4103(08)60264-1.

(16) Schleucher, J.; Sattler, M.; Griesinger, C. Coherence Selection by Gradients without Signal Attenuation: Application to the Three-Dimensional HNCO Experiment. *Angew. Chemie-International Ed. English* **1993**, *32* (10), 1489–1491. https://doi.org/10.1002/anie.199314891.

(17) Palmer, A. G.; Cavanagh, J.; Wright, P. E.; Rance, M. Sensitivity Improvement in Proton-Detected Two-Dimensional Heteronuclear Correlation NMR Spectroscopy. *J. Magn. Reson.* **1991**, *93* (1), 151–170. https://doi.org/10.1016/0022-2364(91)90036-S.

(18) Sattler, M.; Schwendinger, M. G.; Schleucher, J.; Griesinger, C. Novel Strategies for Sensitivity Enhancement in Heteronuclear Multi-Dimensional NMR Experiments Employing Pulsed Field Gradients. *J. Biomol. NMR* **1995**, *6* (1), 11–22. https://doi.org/10.1007/BF00417487.

(19) Cavanagh, J.; Rance, M. Sensitivity Improvement in Isotropic Mixing (TOCSY) Experiments. *J. Magn. Reson.* **1990**, *88* (1), 72–85. https://doi.org/10.1016/0022-2364(90)90109-M.

(20) Cavanagh, J.; Skelton, N.; Fairbrother, W.; Rance, M.; Palmer, A. G. *Protein NMR Spectroscopy: Principles and Practice*, 2nd editio.; Elsevier, Academic Press, 2007.

https://doi.org/10.1016/B978-0-12-164491-8.X5000-3.

(21) Keeler, J.; Neuhaus, D. Comparison and Evaluation of Methods for Two-Dimensional NMR Spectra with Absorption-Mode Lineshapes. *J. Magn. Reson.* **1985**, *63* (3), 454–472. https://doi.org/10.1016/0022-2364(85)90236-7.

(22) Kiihne, S.; Mehta, M. A.; Stringer, J. A.; Gregory, D. M.; Shiels, J. C.; Drobny, G. P. Distance Measurements by Dipolar Recoupling Two-Dimensional Solid-State NMR. *J. Phys. Chem. A* **1998**, *102* (13), 2274–2282. https://doi.org/10.1021/jp9721412.

(23) Oliver, S. L.; Titman, J. J. Isotropic Mixing, Sign Discrimination, and Sensitivity in Solid-State Wideline Heteronuclear Correlation Experiments. *J. Magn. Reson.* **1999**, *140* (1), 235–241. https://doi.org/10.1006/jmre.1999.1844.

(24) Tycko, R. Sensitivity Enhancement in Two-Dimensional Solid-State NMR Spectroscopy by Transverse Mixing. *ChemPhysChem* **2004**, *5* (6), 863–868. https://doi.org/10.1002/cphc.200301208.

(25) Gopinath, T.; Veglia, G. Sensitivity Enhancement in Static Solid-State Nmr Experiments via Singleand Multiple-Quantum Dipolar Coherences. *J. Am. Chem. Soc.* **2009**, *131* (16), 5754–5756. https://doi.org/10.1021/ja900096d.

(26) Gopinath, T.; Traaseth, N. J.; Mote, K.; Veglia, G. Sensitivity Enhanced Heteronuclear Correlation Spectroscopy in Multidimensional Solid-State NMR of Oriented Systems via Chemical Shift Coherences. *J. Am. Chem. Soc.* **2010**, *132* (15), 5357–5363. https://doi.org/10.1021/ja905991s.

(27) Gopinath, T.; Mote, K. R.; Veglia, G. Sensitivity and Resolution Enhancement of Oriented Solid-State NMR: Application to Membrane Proteins. *Prog. Nucl. Magn. Reson. Spectrosc.* **2013**, *75*, 50–68. https://doi.org/10.1016/j.pnmrs.2013.07.004.

(28) Khaneja, N. Sensitivity Enhanced Recoupling Experiments in Solid-State NMR by γ Preparation. *J. Magn. Reson.* **2006**, *183* (2), 242–251. https://doi.org/10.1016/j.jmr.2006.08.017.

(29) Lin, J.; Griffin, R. G.; Khaneja, N. Recoupling in Solid State NMR Using γ Prepared States and Phase Matching. *J. Magn. Reson.* **2011**, *212* (2), 402–411. https://doi.org/10.1016/j.jmr.2011.07.024.

(30) Tošner, Z.; Glaser, S. J.; Khaneja, N.; Nielsen, N. C.; Tosner, Z.; Glaser, S. J.; Khaneja, N.; Nielsen, N. C. Effective Hamiltonians by Optimal Control: Solid-State NMR Double-Quantum Planar and Isotropic Dipolar Recoupling. *J. Chem. Phys.* **2006**, *125* (18). https://doi.org/10.1063/1.2366703.

(31) Ishii, Y. 13C–13C Dipolar Recoupling under Very Fast Magic Angle Spinning in Solid-State Nuclear Magnetic Resonance: Applications to Distance Measurements, Spectral Assignments, and High-Throughput Secondary-Structure Determination. *J. Chem. Phys.* **2001**, *114* (19), 8473–8483. https://doi.org/10.1063/1.1359445.

(32) Khaneja, N.; Reiss, T.; Kehlet, C.; Schulte-Herbruggen, T.; Glaser, S. J. Optimal Control of Coupled Spin Dynamics: Design of NMR Pulse Sequences by Gradient Ascent Algorithms. *J Magn Reson* **2005**, *172* (2), 296–305. https://doi.org/10.1016/j.jmr.2004.11.004.

(33) Bak, M.; Rasmussen, J. T.; Nielsen, N. C. SIMPSON: A General Simulation Program for Solid-State NMR Spectroscopy. *J Magn Reson* **2000**, *147* (2), 296–330. https://doi.org/10.1006/jmre.2000.2179.

(34) Tosner, Z.; Vosegaard, T.; Kehlet, C.; Khaneja, N.; Glaser, S. J.; Nielsen, N. C. Optimal Control in

NMR Spectroscopy: Numerical Implementation in SIMPSON. *J Magn Reson* **2009**, *197* (2), 120–134. https://doi.org/10.1016/j.jmr.2008.11.020.

(35) Tosner, Z.; Andersen, R.; Stevenss, B.; Eden, M.; Nielsen, N. C.; Vosegaard, T.; Stevensson, B.; Eden, M.; Nielsen, N. C.; Vosegaard, T. Computer-Intensive Simulation of Solid-State NMR Experiments Using SIMPSON. *J Magn Reson* **2014**, *246* (0), 79–93. https://doi.org/10.1016/j.jmr.2014.07.002.

(36) Tošner, Z.; Sarkar, R.; Becker-Baldus, J.; Glaubitz, C.; Wegner, S.; Engelke, F.; Glaser, S. J.; Reif, B. Overcoming Volume Selectivity of Dipolar Recoupling in Biological Solid-State NMR Spectroscopy. *Angew. Chemie - Int. Ed.* **2018**, *57* (44), 14514–14518. https://doi.org/10.1002/anie.201805002.

(37) Tošner, Z.; Brandl, M. J.; Blahut, J.; Glaser, S. J.; Reif, B. Maximizing Efficiency of Dipolar Recoupling in Solid-State NMR Using Optimal Control Sequences. *Sci. Adv.* **2021**, *7* (42), 1–11. https://doi.org/10.1126/sciadv.abj5913.

(38) Tošner, Z.; Purea, A.; Struppe, J. O.; Wegner, S.; Engelke, F.; Glaser, S. J.; Reif, B. Radiofrequency Fields in MAS Solid State NMR Probes. *J Magn Reson* **2017**, *284* (Supplement C), 20–32. https://doi.org/https://doi.org/10.1016/j.jmr.2017.09.002.

(39) Akke, M.; Carr, P. A.; Palmer, A. G. Heteronuclear-Correlation NMR Spectroscopy with Simultaneous Isotope Filtration, Quadrature Detection, and Sensitivity Enhancement Using z Rotations. *J. Magn. Reson. Ser. B* **1994**, *104*, 298–302.

(40) Pradhan, T.; Annamalai, K.; Sarkar, R.; Huhn, S.; Hegenbart, U.; Schoenland, S.; Faendrich, M.; Reif, B. Seeded Fibrils of the Germline Variant of Human Lambda-III Immunoglobulin Light Chain FOR005 Have a Similar Core as Patient Fibrils with Reduced Stability. *J. Biol. Chem.* **2020**, *295* (52), 18474–18484. https://doi.org/10.1074/jbc.RA120.016006.

(41) Radamaker, L.; Baur, J.; Huhn, S.; Haupt, C.; Hegenbart, U.; Schönland, S.; Bansal, A.; Schmidt, M.; Fändrich, M. Cryo-EM Reveals Structural Breaks in a Patient-Derived Amyloid Fibril from Systemic AL Amyloidosis. *Nat. Commun.* **2021**, *12* (1), 1–10. https://doi.org/10.1038/s41467-021-21126-2.

(42) Andersen, C. B.; Yagi, H.; Manno, M.; Martorana, V.; Ban, T.; Christiansen, G.; Otzen, D. E.; Goto, Y.; Rischel, C. Branching in Amyloid Fibril Growth. *Biophys. J.* **2009**, *96* (4), 1529–1536. https://doi.org/10.1016/j.bpj.2008.11.024.

(43) Pradhan, T.; Annamalai, K.; Sarkar, R.; Hegenbart, U.; Schoenland, S.; Faendrich, M.; Reif, B. Solid State NMR Assignments of a Human Lambda-III Immunoglobulin Light Chain Amyloid Fibril. *Biomol. NMR Assign.* **2021**, *15* (1), 9–16. https://doi.org/10.1007/s12104-020-09975-2.

(44) Klein, A.; Rovó, P.; Sakhrani, V. V; Wang, Y.; Holmes, J. B.; Liu, V.; Skowronek, P.; Kukuk, L.; Vasa, S. K.; Güntert, P.; Mueller, L. J.; Linser, R. Atomic-Resolution Chemical Characterization of (2x)72-KDa Tryptophan Synthase via Four- and Five-Dimensional 1H-Detected Solid-State NMR. *Proc. Natl. Acad. Sci. U. S. A.* **2022**, *119* (4), e2114690119. https://doi.org/10.1073/pnas.2114690119/-/DCSupplemental.Published.